Belief Function Theory for Intention Estimation for Automated Driving

Xuhui Zhang
Department of Electrical and Computer Engineering, Chair of Automatic Control Engineering (LSR)
Technical University of Munich
Munich, Germany
xuhui.zhang@tum.de

***Abstract*—Interaction with other traffic participants is a quite difficult task in autonomous driving. Much uncertainty comes from multiple possible trajectories and should be considered in motion planning. In this paper, a framework based on belief function theory is proposed to gather information from multiple sources and select the most probable trajectory. First, opinions are generated and fed to this framework. Then, it fuses opinions of independent sources at current time instant, adapts the fused result according to conflict among opinions and updates the belief from the previous time instant with this fused opinion. A prioritization of all possible trajectories is given together with a measure of how much it can be trusted. Crossroad simulations show the functionality of this framework.**

***Index Terms*—belief function theory, belief fusion, intention estimation**

I. Introduction

In recent decades, self-driving cars are a very popular topic and attract the attention of many researchers. Safe automated driving is an important branch of this. Many accidents caused by human errors can be greatly reduced by reliable self-driving systems.

In automated driving, control schemes, such as Model Predictive Control (MPC) are typically used for control and motion planning of the ego vehicle. MPC predicts the behaviour of the ego vehicle over a finite horizon based on constraints. These constraints are set to avoid collision and depend on the motion of target vehicles, cyclists and pedestrians. However, estimating and predicting motion of these traffic participants can be very challenging. First, there can be multiple possible trajectories for target vehicles. Second, cyclists and pedestrians sometimes change their trajectories suddenly and invade the planned path of the ego vehicle.

To estimate behaviors in such situations, a mechanism is required, which includes all possible trajectories and gives each a measure of how likely it is the real one. This measure should be updated as time develops and can be used to select the most probable trajectory. Besides, the confidence level of this estimation should be given to avoid aggressive behaviors of the ego vehicle until the estimation is reliable enough. Based on output of this mechanism, safe motion of the ego vehicle can be planned. To avoid confusion, ego vehicle (EV) refers to the controlled vehicle and target vehicle (TV) represents other traffic participants. Fig 1. demonstrates possible trajectories of two scenarios, namely crossroad and lane change.

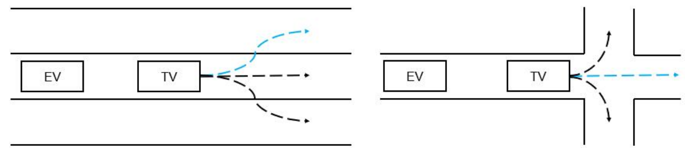

(a) lane change (b) crossroad

Fig. 1: EV has to estimate the behavior of the TV in front of it for its own motion planning. Dashed arrows represent possible trajectories and one of them is the real trajectory (yellow).

II. Related Work

Many previous works have proposed various methods to estimate behaviors of traffic participants. [1] introduces a lane change detection mechanism, which divides the whole process into four phases and estimates the intention in each phase. But this method relies on phase models of lane change and is not general enough. In [2], Interacting Multiple Model Kalman Filter (IMM-KF) is used to estimate and predict positions of target vehicles. However, the uncertainty is propagated only along with the trajectory with the highest probability. [3] improves the method based on IMM-KF by including all possible trajectories in the prediction horizon. Different from IMM-KF, which is based on probability [4], belief function theory allows giving a subjective measure for how much an opinion can be trusted.

In [5], belief function theory is utilized for sensor fusion. Observations of independent sensors are fused with Dempster-Shafer evidence combination rules and an improved evidence combination rules based on this. The former trusts sensors of different qualities equally, which gives worse result with noisy sensors added. The latter introduces weight for each sensor. However, conflict among observations is not dealt with. The result becomes more certain with more observations, even when they do not agree with each other. [6] proposes several conflict detection mechanisms. However, uncertainty is not included in these mechanisms. This means two confident opinions have the same degree of conflict as two uncertain opinions with the same belief distribution difference, which is to some extent unreasonable. [7] develops a conflict handling mechanism, called Uncertainty Maximization (UM). UM transfers the maximal amount from belief masses to uncertainty independent of the degree of conflict. Such increase of uncertainty can be too much for small conflict.

III. Modeling of Dynamics

In this work, the scenario of target vehicles at crossroad is studied. Other scenarios of cyclists and pedestrians are similar, but will not be discussed out of simplicity.

For generation of possible trajectories, a dynamic model for target vehicles is required. Adapted from [8], the linear, discrete-time point-mass model for target vehicles is given by

$$\boldsymbol{\xi}_{k+1}^{\mathrm{TV}} = \boldsymbol{A}\boldsymbol{\xi}_k^{\mathrm{TV}} + \boldsymbol{B}\boldsymbol{u}_k^{\mathrm{TV}} \tag{1}$$

$$\boldsymbol{u}_k^{\mathrm{TV}} = \widetilde{\boldsymbol{u}}_k^{\mathrm{TV}} + \boldsymbol{w}_k^{\mathrm{TV}} \tag{2}$$

where $\boldsymbol{\xi}_k^{\mathrm{TV}} = [x_k^{\mathrm{TV}}, v_{x,k}^{\mathrm{TV}}, y_k^{\mathrm{TV}}, v_{y,k}^{\mathrm{TV}}]^\top$ denotes the state of this target vehicle, namely longitudinal position and velocity x_k^{TV} and $v_{x,k}^{\mathrm{TV}}$ together with lateral position and velocity y_k^{TV} and $v_{y,k}^{\mathrm{TV}}$. The system matrix and the input matrix are respectively

$$\boldsymbol{A} = \begin{bmatrix} 1 & T & 0 & 0 \\ 0 & 1 & 0 & 0 \\ 0 & 0 & 1 & T \\ 0 & 0 & 0 & 1 \end{bmatrix}, \quad \boldsymbol{B} = \begin{bmatrix} 0.5T^2 & 0 \\ T & 0 \\ 0 & 0.5T^2 \\ 0 & T \end{bmatrix} \tag{3}$$

where T is the sampling time. Here a feedback controller for reference tracking is given by

$$\widetilde{\boldsymbol{u}}_k^{\mathrm{TV}} = \boldsymbol{K}(\boldsymbol{\xi}_k^{\mathrm{TV}} - \boldsymbol{\xi}_{\mathrm{ref},k}^{\mathrm{TV}}) \tag{4}$$

where $\boldsymbol{\xi}_{\mathrm{ref},k}^{\mathrm{TV}}$ is the reference state. The feedback matrix $\boldsymbol{K}$ is calculated based on linear-quadratic regulator policy. The input perturbation is assumed to be Gaussian distributed with $\boldsymbol{w}_k^{\mathrm{TV}} \sim \mathcal{N}(0, \boldsymbol{\Sigma}_w^{\mathrm{TV}})$.

To make application scenarios close to reality, the approach is based on noisy measurements of the state, i.e.,

$$\widetilde{\boldsymbol{\xi}}_k^{\mathrm{TV}} = \boldsymbol{\xi}_k^{\mathrm{TV}} + \boldsymbol{w}_k^{\mathrm{sens}} \tag{5}$$

where $\widetilde{\boldsymbol{\xi}}_k^{\mathrm{TV}}$ denotes the measured state at time instant k. The sensor noise is assumed to be truncated Gaussian noise, which is denoted by $\boldsymbol{w}_k^{\mathrm{sens}} \sim \mathcal{N}(0, \boldsymbol{\Sigma}_w^{\mathrm{sens}})$.

IV. Overview of the Approach

The approach utilized in this work can be divided into three parts, namely generation of opinions, multi-source information fusion and belief distribution update. In the first part, information is collected from all possible sources, like measured states, traffic light and turn signals. Then an opinion, which is embodied as a vector containing belief mass for each possibility and uncertainty, is generated for each source. Here possibilities can be understood as possible trajectory of the target vehicle. The combination of the last two parts is the belief processing framework, which works independently of how opinions are generated. The belief mass of the most probable possibility tends to be dominant and uncertainty decreases to a relatively small value in the output of this framework. In Fig. 2, the basic structure of this framework and the information flow in this approach are demonstrated.

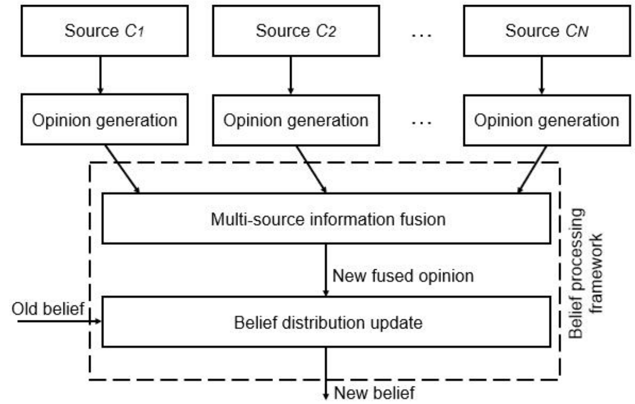

Fig. 2: Basic structure and information flow. Here a source can be measured states, traffic light or turn signal. Multi-source information fusion deals with opinions of different sources at the same time instant. Belief distribution update starts with an initial belief distribution, which develops as time goes.

V. Generation of Opinions

In this section, a brief introduction to belief function theory will be given first, followed by examples of how opinions are generated from measured states and turn signal.

A. Belief Function Theory

Belief function theory can be understood as a generalization of Bayesian theory. One major difference is that support can be assigned not only to each singleton but the union of several singletons [9]. For instance, a singleton is "the target vehicle is turning left" while a union is "the target is either turning left or turning right".

Assigned supports to singletons and unions are called belief masses, which sum up to one. The belief mass assigned to the largest union including all singletons is called uncertainty [7]. Uncertainty is inversely proportional to the subjective confidence of this opinion.

In the crossroad scenario, an opinion is embodied as $\boldsymbol{\omega}^{C_i} = [b(x_{\mathrm{l}}^{C_i}), b(x_{\mathrm{s}}^{C_i}), b(x_{\mathrm{r}}^{C_i}), \mu^{C_i}]^\top$, where x_{l}, x_{s} and x_{r} denote "turning left", "straight" and "turning right" respectively. b is the corresponding belief mass while μ^{C_i} is the uncertainty. C_i indicates the source of this opinion.

B. Opinion Generation from Measured States

When there are no input noise and sensor noise, the measured state should completely agree with the real trajectory's state. However, they are still different due to noises. When trajectories becomes divided, the measured state is assumed to be closer to the state of the real one. Opinion is generated based on comparison between the state of each possible trajectory and the measured state.

Given dynamic model (1) and (2) of the target vehicle together with reference state $\boldsymbol{\xi}_{\mathrm{ref},k}^{\mathrm{TV}}$ for tracking, states $\boldsymbol{\xi}_{\mathrm{l},k}^{\mathrm{TV}}$, $\boldsymbol{\xi}_{\mathrm{s},k}^{\mathrm{TV}}$ and $\boldsymbol{\xi}_{\mathrm{r},k}^{\mathrm{TV}}$ can be obtained for all possible trajectories. To obtain this, input noise $\boldsymbol{w}_k^{\mathrm{TV}}$ and sensor noise $\boldsymbol{w}_k^{\mathrm{sens}}$ are set to zero. At each time instant, the state of the real trajectory is given by the sensor, e.g., $\widetilde{\boldsymbol{\xi}}_k^{\mathrm{TV}} = [\widetilde{x}_k^{TV}, \widetilde{v}_{x_k}^{TV}, \widetilde{y}_k^{TV}, \widetilde{v}_{y_k}^{TV}]^\top$. Both input noise $\boldsymbol{w}_k^{\mathrm{TV}}$ and sensor noise $\boldsymbol{w}_k^{\mathrm{sens}}$ are included.

Each component of the state vector can be considered as an independent source. The selection of state component for opinion generation is based on the specific scenario. First, we compare the measured state and the ideal state of each trajectory, e.g., $\tilde{y}_k^{\mathrm{TV}} - y_{1,k}^{\mathrm{TV}}$. Under the assumption of Gaussian noises, the distribution of the measured state is also be Gaussian around the ideal state of the real trajectory. This means that the closer the measured state and the ideal state of one trajectory are, the more likely this trajectory is the real trajectory. Based on this, probability density function of Gaussian distribution (Gaussian PDF) is used to set the belief mass of each trajectory, i.e.,

$$b_k(x_j^{C_i}) = \frac{1}{\sigma_j\sqrt{2\pi}} e^{-\frac{1}{2}(\frac{\tilde{y}_k^{\mathrm{TV}} - y_{j,k}^{\mathrm{TV}}}{\sigma_j})^2}, \quad j = \mathrm{l}, \mathrm{s}, \mathrm{r} \tag{6}$$

$$\boldsymbol{b}_k(x^{C_i}) = [b_k(x_{\mathrm{l}}^{C_i}), b_k(x_{\mathrm{s}}^{C_i}), b_k(x_{\mathrm{r}}^{C_i})]^\top \tag{7}$$

where σ_j depends on input noise and sensor noise of each trajectory. In (7), vector $\boldsymbol{b}_k(x^{C_i})$ containing all belief masses is the belief distribution at time instant k. Even if the measured state is far from the ideal state of one trajectory, it could still be the real one due to very larger noise. Larger noise makes the measured state more distributed while smaller noise results in more concentrated measured state. The comparison is demonstrated in Fig. 3.

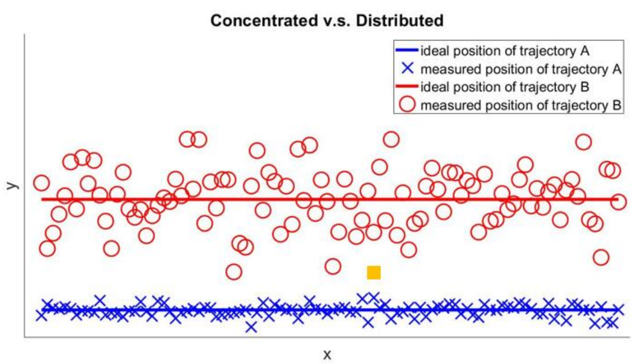

Fig. 3: The noise of trajectory A (red) is quite large with a standard deviation of 0.7 while the noise of trajectory B (blue) is rather small with a standard deviation of 0.1. The measured position (marked as yellow box) is closer to the ideal position of trajectory A. However, this measured state seems more likely to belong to trajectory B because of the large noise.

For further step of setting uncertainty, vector $\boldsymbol{b}_k(x^{C_i})$ has to be normalized by

$$\boldsymbol{b}_k(x^{C_i}) = \frac{\boldsymbol{b}_k(x^{C_i})}{||\boldsymbol{b}_k(x^{C_i})||_1}. \tag{8}$$

This makes belief masses of all possible trajectories sum up to one. Since uncertainty is not included yet, they can also be regarded as probabilities.

Since uncertainty is a subjective measure, there is no unique method for setting it. In this work, the method based on perturbation of previous belief distributions is proposed with

$$\mu_k^{C_i} = \frac{1}{2(N-1)} \sum_{i=k-N+2}^{k} ||\boldsymbol{b}_i(x^{C_i}) - \boldsymbol{b}_{i-1}(x^{C_i})||_1 \tag{9}$$

where k is the current time instant and N is the window size. The summation term records how much the belief distribution changes from one time instant to the next over the time period of N . A larger perturbation of the belief distribution reflects worse reliability of the source, which means this source should be trusted less. An interpretation of this can be found in Fig. 4. This corresponds to the functionality of uncertainty.

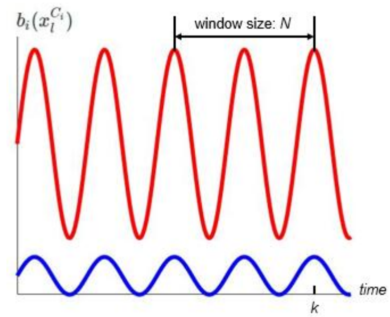

Fig. 4: Development of the belief over time. Larger perturbation of belief mass (red) should result in higher uncertainty than smaller perturbation (blue).

For N time instants, $(N-1)$ comparisons can be made. The potential largest change of belief distribution can be found in the case $\boldsymbol{b}_{i-1}(x^{C_i}) = [1, 0, 0]^\top$ and $\boldsymbol{b}_i(x^{C_i}) = [0, 0, 1]^\top$. Corresponding $||\boldsymbol{b}_i(x^{C_i}) - \boldsymbol{b}_{i-1}(x^{C_i})||_1$ is 2. $\frac{1}{2(N-1)}$ in (9) normalizes the sum of perturbation by the theoretically largest sum, which guarantees $\mu_k^{C_i} \in [0, 1]$.

For comparison of two belief distributions, they have to reach the same scale. This is made by normalization in (8). Now all components of the opinion are determinate. To guarantee the sum of all belief masses and uncertainty equal to one, the opinion is set to

$$\boldsymbol{\omega}_k(x^{C_i}) = [(1 - \mu_k^{C_i})\boldsymbol{b}_k(x^{C_i}), \mu_k^{C_i}]^\top \tag{10}$$

C. Opinion Generation from Turn Signal

An Additional opinion comes from the turn signal. When the TV is approaching the crossroad, the opinion based on the turn signal can be generated. If the turn signal is given correctly, it should consist with the trajectory it is going to take afterwards. A very large belief mass is assigned to this trajectory with low uncertainty, e.g.,

$$\boldsymbol{\omega}_k^{\mathrm{turn}} = [0.7, 0, 0, 0.3]^\top, \quad k \in [k_{\mathrm{start}}, k_{\mathrm{end}}] \tag{11}$$

where k_{start} and k_{end} are start time and end time of turn signal.

VI. Belief Processing Framework

In belief processing framework, a fused opinion at current time instant is generated to combine opinions given by different sources, adaptation is made based on conflict among opinions and belief at previous time instant is updated with this fused opinion. Two related fusion operators and a conflict detection mechanism are introduced.

A. Multi-Source Information Fusion

1) Cumulative Belief Fusion Operator: Until now, opinions are gathered from all available sources at each time instant.

As shown in Fig. 5, Cumulative Belief Fusion operator (CBF) is utilized to combine them together and generate an overall opinion at current time instant. According to [7], the fused opinion of CBF is expressed as:

$$Case\ 1: \mu_k^{C_i} \neq 0,\ \forall i$$

$$b_k^{\text{fo}}(x) = \frac{\sum_{i=1}^{N}(b_k(x^{C_i})\prod_{j\neq i}^{N}\mu_k^{C_j})}{\sum_{i=1}^{N}(\prod_{j\neq i}^{N}\mu_k^{C_j}) - (N-1)\prod_{i=1}^{N}\mu_k^{C_i}} \tag{12}$$

$$\mu_k^{\text{fo}} = \frac{\prod_{i=1}^{N}\mu_k^{C_i}}{\sum_{i=1}^{N}(\prod_{j\neq i}^{N}\mu_k^{C_j}) - (N-1)\prod_{i=1}^{N}\mu_k^{C_i}} \tag{13}$$

$$Case\ 2: \exists \mu_k^{C_i} = 0,\ \text{define}\ I = \{i|\mu_k^{C_i} = 0\}$$

$$b_k^{\text{fo}}(x) = \frac{1}{N^I}\sum_{i=1}^{N^I} b_k(x^{C_i}),\ i \in I; \quad \mu_k^{\text{fo}} = 0 \tag{14}$$

where N is the total number of opinions and N_I is the number of opinions, whose uncertainty is zero. In (12) and (14), $b_k^{\text{fo}}(x)$ stands for belief mass of each possible outcome, namely $b_k^{\text{fo}}(x_{\text{l}})$, $b_k^{\text{fo}}(x_{\text{s}})$ and $b_k^{\text{fo}}(x_{\text{r}})$. Operation with CBF is written as $\boldsymbol{\omega}_k^{\text{fo}} = \bigcup_{\text{CBF}}\{\boldsymbol{\omega}_k^{C_1}, ..., \boldsymbol{\omega}_k^{C_N}\}$, where $\boldsymbol{\omega}_k^{\text{fo}} = [\boldsymbol{b}_k^{\text{fo}}(x), \mu_k^{\text{fo}}]^\top$ is the fused opinion.

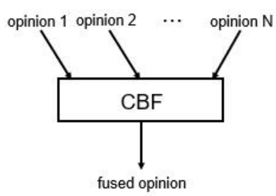

Fig. 5: CBF combines opinions given by different sources at current time instant.

(14) gives fused result of the extreme case, in which more than one opinion is 100% confident. All these opinions are averaged to obtain the result while the other opinions are ignored due to less confidence.

An important feature of CBF operation is that the more opinions it fuses, the smaller the uncertainty is and the larger belief masses are. For fusion of opinions at the same time instant, what happens in reality should be better exposed, if there are more opinions of independent sources. Since all opinions describe the same phenomenon, more information helps people get close to the truth. This is realized by CBF's feature that fusion with more opinions increases belief masses and decreases the uncertainty. Such consideration is valid for consistent opinions.

2) Conflict Detection and Handling: For conflicting opinions, decreasing uncertainty after fusion with CBF is not reasonable. Here conflicting opinions mean belief distributions that do not agree with each other. To deal with this issue, a conflict detection and handling mechanism (CDH) is utilized to detect how much the conflict among these opinions is and transfer part of each belief masses to the uncertainty.

Before fusion, we go through each pair of opinions and calculate degree of conflict with

$$\text{doc}_{ij} = \frac{1}{2}\left\|\frac{\boldsymbol{b}_k^{C_i}}{||\boldsymbol{b}_k^{C_i}||_1} - \frac{\boldsymbol{b}_k^{C_j}}{||\boldsymbol{b}_k^{C_j}||_1}\right\|_1 \sqrt{(1-\mu^{C_i})(1-\mu^{C_j})} \tag{15}$$

where $\boldsymbol{b}_k^{C_i}$ and $\boldsymbol{b}_k^{C_j}$ are belief distributions of opinions $\boldsymbol{\omega}_k^{C_i}$ and $\boldsymbol{\omega}_k^{C_j}$ respectively. The term inside $||\cdot||_1$ describes the difference between belief distributions. If these two distributions do not agree with each other and both opinions have very high confidence, the degree of conflict should be higher than two less confident opinions with the same difference of belief distributions. This explains multiplication with geometric mean of $1-\mu$ in (15).

It has to be noticed that ratio of belief masses rather than values matters in the comparison. For instance, $\boldsymbol{b}_1(x^{C_i}) = [0.1, 0.1, 0.2]^\top$ and $\boldsymbol{b}_2(x^{C_i}) = [0.2, 0.2, 0.4]^\top$ are considered as the same belief distribution, since both ratios of belief masses are 1:1:2. This represents consistency of two belief distributions. Uncertainty does not play a role in the comparison of belief distribution, since it only scales belief masses. Such consideration shows the reason why $\boldsymbol{b}_k(x^{C_i})$ is normalized in (15) before calculating difference.

In order to know the original result of CBF, conflict is handled after CBF operation rather than before. Fused opinion is adapted based on degree of conflict with

$$\boldsymbol{b}_k^{\text{fo}}(x) = (\prod(1-doc_{ij}))^{\frac{1}{n}}\boldsymbol{b}_k^{\text{fo}}(x) \tag{16}$$

$$\mu_k^{\text{fo}} = 1 - ||\boldsymbol{b}_k^{\text{fo}}(x)||_1 \tag{17}$$

where n is the number of pairs of opinions. The more conflict there is, the more belief masses should be transferred to uncertainty, which is shown in (16).

B. Belief Distribution Update

1) Weighted Belief Fusion Operator: After the processing above, fused opinion containing all information at current time instant is obtained. This opinion can be utilized for updating belief distribution from previous time instant, which is shown in Fig. 6. This can be realized by Weighted Belief Fusion operator (WBF). Given by [7], the fused result of WBF is obtained by

$$Case\ 1: \mu_{k-1}^{\text{ub}} \neq 0,\ \mu_k^{\text{fo}} \neq 0$$

$$b_k^{\text{ub}}(x) = \frac{b_{k-1}^{\text{ub}}(1-b_{k-1}^{\text{ub}})\mu_k^{\text{fo}} + b_k^{\text{fo}}(1-b_k^{\text{fo}})\mu_{k-1}^{\text{ub}}}{\mu_{k-1}^{\text{ub}} + \mu_k^{\text{fo}} - 2\mu_{k-1}^{\text{ub}}\mu_k^{\text{fo}}} \tag{18}$$

$$\mu_k = \frac{(2-\mu_{k-1}^{\text{ub}} + \mu_k^{\text{fo}})\mu_{k-1}^{\text{ub}}\mu_k^{\text{fo}}}{\mu_{k-1}^{\text{ub}} + \mu_k^{\text{fo}} - 2\mu_{k-1}^{\text{ub}}\mu_k^{\text{fo}}} \tag{19}$$

$$Case\ 2: \exists \mu_i = 0,\ \mu_i \in \{\mu_{k-1}^{\text{ub}}, \mu_k^{\text{fo}}\},\ b_i \in \{b_{k-1}^{\text{ub}}, b_k^{\text{fo}}\}$$

$$b_k^{\text{ub}}(x) = \frac{1}{N_I}\sum_{i=1}^{N_I} b_i,\ \forall i \in I,\ \mu_k^{\text{ub}} = 0 \tag{20}$$

$$Case\ 3: \mu_{k-1}^{\text{ub}} = 1,\ \mu_k^{\text{fo}} = 1$$

$$b_k^{\text{ub}}(x) = 0;\ \mu_k^{\text{ub}} = 1 \tag{21}$$

where I corresponds to the union of belief at $k-1$ and fused opinion at k with zero uncertainty. WBF can be applied for more general case with N beliefs. For the application of updating belief, N should be 2, namely belief at previous time instant and fused opinion at current time instant.

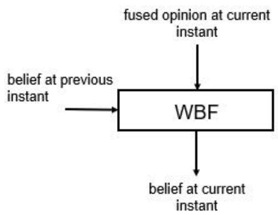

Fig. 6: WBF updates belief from previous time instant with the fused opinion at current time instant.

In (18), (20) and (21), $b_k^{\text{ub}}(x)$ stands for belief mass of each possible outcome, namely $b_k^{\text{ub}}(x_l)$, $b_k^{\text{ub}}(x_s)$ and $b_k^{\text{ub}}(x_r)$. To represent operation with WBF, $\boldsymbol{\omega}_k^{\text{ub}} = \bigcup_{\text{WBF}}\{\boldsymbol{\omega}_{k-1}^{\text{fo}}, \boldsymbol{\omega}_k^{\text{ub}}\}$ is used. $\boldsymbol{\omega}_k^{\text{ub}} = [\boldsymbol{b}_k^{\text{ub}}(x), \mu_k^{\text{ub}}]^\top$ is the updated belief.

The major difference between CBF and WBF is that the uncertainty given by WBF operator is between two uncertainties fed to WBF while the uncertainty given by CBF operator is smaller than the minimal uncertainty of all sources. Different from CBF, belief at $k-1$ and fused opinion at k describes two different things. As the real trajectory of TV develops, intentions at $k-1$ and at k can be different and belief can also change from time to time. For instance, the uncertainty should increase if the TV switch from one trajectory to another. Updating belief with CBF will still decrease the uncertainty, which makes it not a reasonable choice. For this case, WBF is more suitable than CBF. WBF makes compromise between belief at $k-1$ and fused opinion at k. Both accumulated information and new opinion are considered. If the fused opinion remains the same for a time period, the fused result given by WBF converges to the fused opinion. This means the TV has stayed on the same trajectory for some time. Features of CBF, CDH and WBF can be better understood with examples in Table I, where the first two components of each vector are belief masses of corresponding possibilities and the last component is uncertainty. $\boldsymbol{b}_1$ and $\boldsymbol{b}_2$ are two quite conflicting beliefs. The uncertainty given by CBF always decreases with more beliefs. That given by WBF remains the same, since all beliefs for fusion have the same uncertainty. Due to conflict between $\boldsymbol{b}_1$ and $\boldsymbol{b}_2$, the uncertainty increases after CDH is conducted. However, such increase becomes more unremarkable, as more $\boldsymbol{b}_2$ are added. With 8 $\boldsymbol{b}_2$, the fused result given by WBF is already very close to $\boldsymbol{b}_2$.

Table I: Fused results of the same belief set with different fusion operators. Here $\boldsymbol{b}_1$ = [0.5, 0.1, 0.4] and $\boldsymbol{b}_2$ = [0.1, 0.5, 0.4]

	CBF	CBF-CDH	WBF
1 $\boldsymbol{b}_1$ with 1 $\boldsymbol{b}_2$	[0.375, 0.375, 0.250]	[0.225, 0.225, 0.550]	[0.300, 0.300, 0.400]
1 $\boldsymbol{b}_1$ with 2 $\boldsymbol{b}_2$	[0.318, 0.500, 0.182]	[0.226, 0.356, 0.418]	[0.200, 0.400, 0.400]
1 $\boldsymbol{b}_1$ with 8 $\boldsymbol{b}_2$	[0.224, 0.707, 0.069]	[0.200, 0.631, 0.169]	[0.102, 0.498, 0.400]

With information at current time instant, the updated belief can adapt to the switch among trajectories quite well. When a switch happens, only some time is needed for the dominant belief mass to follow the new trajectory and for the uncertainty to decrease to a relatively small value. This agrees with the role of uncertainty in motion planning. Too aggressive behavior can be avoided when a switch is happening and the uncertainty is not small enough.

VII. Simulation Results

To validate the functionality of this approach, the crossroad scenario is simulated. For each simulation, the real trajectory of TV is selected in advance and the measured state at each time instant is generated based on this. In all simulations below components of $\boldsymbol{\omega}_k^{\text{fo}}$ is plotted over time. The belief distribution is initialized as $\boldsymbol{\omega}_{k=0}^{\text{fo}} = [0.03, 0.03, 0.03, 0.9]^\top$. Here the sampling time T is set to 0.01 second. Noises are set with $\boldsymbol{\Sigma}_w^{\text{TV}} = \begin{bmatrix} 0.1 & 0 & 0 & 0 \\ 0 & 0.1 & 0 & 0 \\ 0 & 0 & 0.1 & 0 \\ 0 & 0 & 0 & 0.1 \end{bmatrix}$ and $\boldsymbol{\Sigma}_w^{\text{sens}} = \begin{bmatrix} \sigma_x & 0 & 0 & 0 \\ 0 & \sigma_{v_x} & 0 & 0 \\ 0 & 0 & \sigma_y & 0 \\ 0 & 0 & 0 & \sigma_{v_y} \end{bmatrix}$.

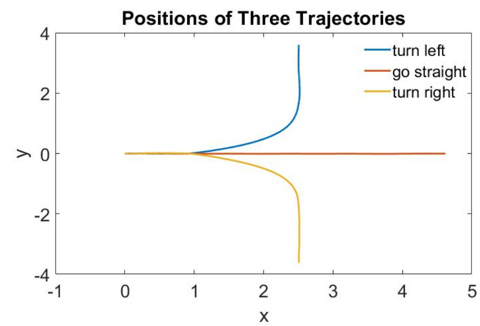

(a)

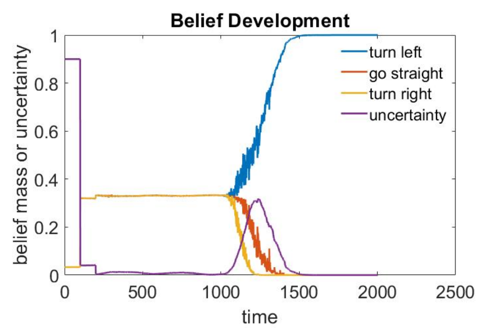

(b)

Fig. 7: Result of one source based on measured y. The real trajectory of TV is "turn left". TV starts to turn at t = 1000. σ_y is 0.1.

In Fig. 7, belief masses of all possible trajectories are equal and uncertainty is very small for t $\in$ [0, 1000]. This is because these three trajectories are not divided in this time period. The measured y value is equally likely to belong to all these three trajectories. The belief distribution remains almost unchanged during this time. When trajectories become divided, measured y value is closer to ideal y value of the real trajectory. This explains the increase of belief mass "turn left" and the decrease of the others. However, such increase and decrease lead to the change of belief distribution especially when the division starts. This results in the increase of uncertainty. When the turn is almost finished, belief mass of "turn left" becomes dominant and this belief distribution will be kept. This reduces the uncertainty to almost 0.

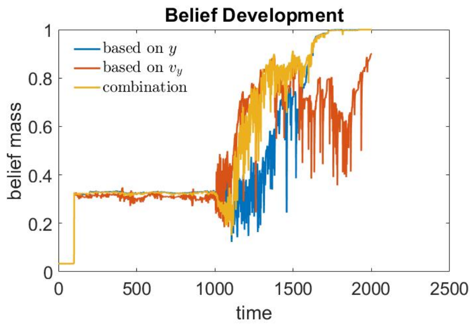

(a)

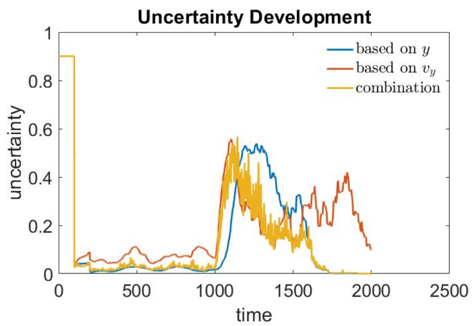

(b)

Fig. 8: Result of one source based on measured y and the other source based on measured v_y. The real trajectory of TV is "turn left". TV starts to turn at t = 1000. σ_y is 0.4 and σ_{v_y} is 0.1.

In simulation of Fig. 8, a sensor of better quality is utilized to measure v_y while a sensor of worse quality to measure y. The scenario is simulated with two sources respectively and with the combination of them. It has to be mentioned that the TV keeps a constant v_y in trajectories of "turn left" and "turn right" after the turn is finished. This makes belief mass of the real trajectory not that dominant and the uncertainty not fully vanished in the opinion based on measured v_y. But due to smaller sensor noise, belief mass of the real trajectory tends to increase faster in this opinion. In the result of combination, both belief mass of the real trajectory and the uncertainty are closer to these of opinion based on measured v_y when the division starts. At the end of the turn, they almost agree with these of opinion based on measured y. This comes from the property of CBF. A more reliable source during a specific time tends to have smaller uncertainty. The fused result of CBF is closer to the opinion of this source. Advantages of different sources can be combined.

Fig. 9 demonstrates the result of an additional source based on turn signal. Belief masses are equal in this opinion before division. The real trajectory is given large preference when the division starts. Turn signal is assumed to have a strong opinion, which reduces the time for convergence (belief mass of the real trajectory to 1 and uncertainty to 0). When the turn starts, uncertainty increases suddenly to a large value. This is because the source based on y just starts to give more preference to the real trajectory. This leads to conflict with that given by turn signal, which vanished after some time.

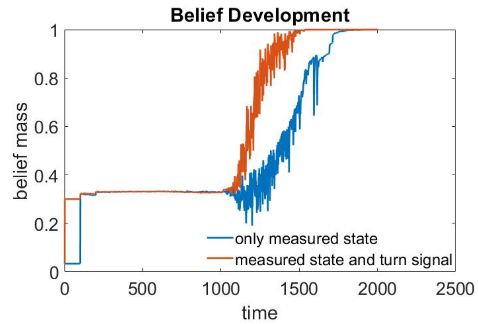

(a)

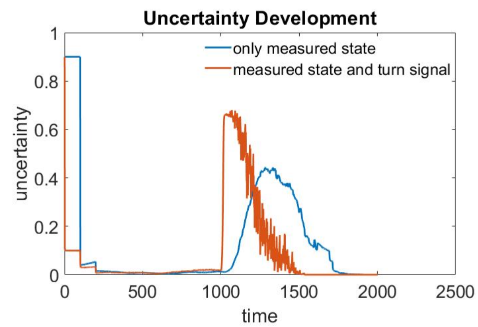

(b)

Fig. 9: Result of one source based on measured y and the other source based on turn signal. The real trajectory of TV is "turn left". TV starts to turn at t = 1000. σ_y is 0.3. Opinion based on turn signal is $[0.3, 0.3, 0.3, 0.1]^\top$, t $\in$ [0, 1000] and $[1, 0, 0, 0]^\top$, t $\in$ [1001, 2000].

With turn signal, earlier judgement can be made.

In simulation of Fig. 10, a source gives faulty information for some time. Faulty information refers to rather large preference to a wrong trajectory, e.g., "turn right" here. At the beginning of the turn, belief mass of the real trajectory decreases while uncertainty increases suddenly due to the conflict brought by the faulty information. When it ends, opinions of two sources agree with each other and the uncertainty of the fused opinion given by CBF is small. This makes WBF rely more on the fused opinion rather than the accumulated belief distribution and the new belief distribution becomes closer to the reality with only more time for convergence. Such result shows the robustness of this framework.

VIII. Conclusion

Through theoretical discussion and simulation results, we find that this approach is qualified for the behavior estimation task when there are multiple possible trajectories. The belief processing framework can be applied for more general cases, lane change and overtake. It works independently from opinion generation. For each specific case, sources should be chosen properly. With information given by them, trajectories should be distinguished. The output of this framework can be utilized for motion planning to combine safety and efficiency.

One problem with this framework is the perturbation in the fused result. Due to noises, belief masses and uncertainty of each opinion can have some perturbation. Such perturbation

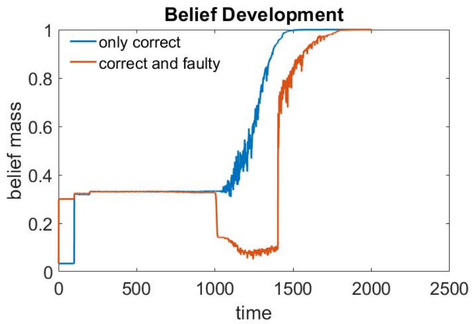

(a)

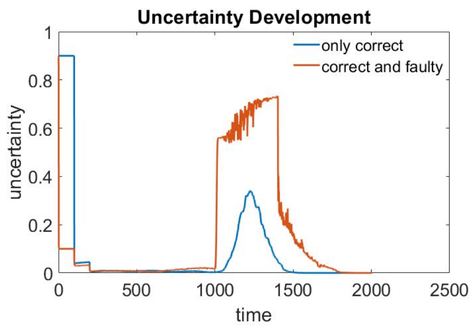

(b)

Fig. 10: Result of one source based on measured y and the other source with faulty information. The real trajectory of TV is "turn left". TV starts to turn at t = 1000. σ_y is 0.1. Opinion with faulty information is $[0.3, 0.3, 0.3, 0.1]^\top$, t $\in$ [0, 1000], $[0, 0, 0.7, 0.3]^\top$, t $\in$ [1001, 1400] and $[0.7, 0, 0, 0.3]^\top$, t $\in$ [1401, 2000].

is strengthened after operation with both CBF and WBF. As uncertainty plays the role of weight in both fusion operators, more stable uncertainty can help to solve this problem. A new mechanism of setting uncertainty can be developed for improvement.

Now this framework can only select the real trajectory from all possible ones but cannot update the estimation of the real trajectory's state based on measurement. IMM-KF combines Bayes' theorem and Kalman Filter [4]. It can manage selection and estimation based on probability. Inspired by this, a further step can be the combination of this framework and Kalman Filter. The updated estimate of real trajectory's state can be given for better planning.

References

[1] H. Woo, Y. Ji, H. Kono, Y. Tamura, Y. Kuroda, T. Sugano, Y. Yamamoto, A. Yamashita, and H. Asama, "Lane-change detection based on vehicle-trajectory prediction," *IEEE Robotics and Automation Letters*, vol. 2, no. 2, pp. 1109–1116, 2017.

[2] A. Carvalho, Y. Gao, S. Lefevre, and F. Borrelli, "Stochastic predictive control of autonomous vehicles in uncertain environments," in *12th International Symposium on Advanced Vehicle Control*, pp. 712–719, 2014.

[3] A. Muraleedharan, A.-T. Tran, H. Okuda, and T. Suzuki, "Scenario-based model predictive speed controller considering probabilistic constraint for driving scene with pedestrian," in *2020 IEEE 23rd International Conference on Intelligent Transportation Systems (ITSC)*, pp. 1–7, IEEE, 2020.

[4] M. E. Farmer, R.-L. Hsu, and A. K. Jain, "Interacting multiple model (imm) kalman filters for robust high speed human motion tracking," in *Object recognition supported by user interaction for service robots*, vol. 2, pp. 20–23, IEEE, 2002.

[5] H. Wu, M. Siegel, R. Stiefelhagen, and J. Yang, "Sensor fusion using dempster-shafer theory [for context-aware hci]," in *IMTC/2002. Proceedings of the 19th IEEE Instrumentation and Measurement Technology Conference (IEEE Cat. No. 00CH37276)*, vol. 1, pp. 7–12, IEEE, 2002.

[6] A. Martin, "Conflict management in information fusion with belief functions," in *Information quality in information fusion and decision making*, pp. 79–97, Springer, 2019.

[7] A. Jøsang, "Categories of belief fusion," *J. Adv. Inf. Fusion*, vol. 13, no. 2, pp. 235–254, 2018.

[8] T. Brüdigam, M. Olbrich, D. Wollherr, and M. Leibold, "Stochastic model predictive control with a safety guarantee for automated driving," *IEEE Transactions on Intelligent Vehicles*, 2021.

[9] R. P. Srivastava, "An introduction to evidential reasoning for decision making under uncertainty: Bayesian and belief function perspectives," *International Journal of Accounting Information Systems*, vol. 12, no. 2, pp. 126–135, 2011.